



## Calculations of Muon Radiation for the Meson area

April, 1980

A. Wehmann

### Abstract

The muon radiation pattern produced by protons striking the M-center target has been studied at some length--using the C.E.R.N. computer program "HALO" (Ref. 1 ). The purpose of these studies has been to gain insight into the muon radiation pattern likely when targetting 1000 Gev protons. In the studies to-date positive pion production at the target is followed by decay and transport of the resulting muons through an approximation to the Meson area tunnels and shielding. The resulting radiation density is very sensitive to the presence of magnetic field in the first M2 bending magnets. Levels calculated due to  $\pi^+ \rightarrow \mu^+ \nu$  decay are  $\sim 0.3$  mr/hr (  $\sim 1.4$  mr/hr ) for  $10^{12}$  400 Gev/c protons (1000 Gev protons) interacting in the target.

## Introduction

A prior study of muon fluxes in the Meson experimental area was made by T. Ferbel; it is described in Volume 2 of the 1976 Fermilab Summer Study. In comparing 1000 Gev production to 400 Gev production, a prediction of an increase by a factor of 100 was made. For  $3 \times 10^{12}$ , 400 Gev protons on a 20 cm Be target the muon flux density in a 4 mr cone about the direction of the primary proton beam was calculated to be  $1.5 \times 10^5 \mu / \text{sq. meter}$  ( $\sim .2 \text{ mr/hr}$  for a 1976 accelerator cycle time of 8 sec). This 1976 report has served as a starting point for the present study. We have proceeded from it to include the effect of magnetic field downstream of the target; we have used a Monte-Carlo approach rather than a closed-form calculation; we have tried another production model; and we have more accurately approximated the shielding material and voids. Left for later study are: (1) "direct" muon production, (2) effects due to primary-energy protons striking material downstream of the target, (3) variations of the magnetic field arrangement downstream of the target, (4) refinements to the representation of the passive shielding in the area, and (5) investigation of other possible production models. Other topics for study would be the muons resulting from interactions in the M-West target and the muons that would result from targetting for the M1 High Intensity Pion beam.

## Review of 1976 Ferbel Summer Study

In the course of the Ferbel Summer Study fits to  $\pi^+$ ,  $\pi^-$ ,  $K^+$ , &  $K^-$  production data were made to cover the  $x$  (Feynman  $x$ ) region of interest and these were used to calculate the number of decay muons above 200 Gev in energy. An estimate for multiple scattering was made in order to calculate the area density of these muons in the region of the M3 experiments. A 20 cm Be target was used--followed by a 5 meter decay path.

The production cross sections used were

$$\frac{d\sigma}{dx}(\pi^+) = 2.5 \frac{d\sigma}{dx}(\pi^-)$$

$$\frac{d\sigma}{dx}(K^+) = 2 \frac{d\sigma}{dx}(K^-)$$

and

$$\frac{d\sigma}{dx} (\pi^-) = 250 e^{-11x} \text{ mb}$$

$$\frac{d\sigma}{dx} (K^-) = 22 e^{-10x} \text{ mb}$$

both for  $x > 0.2$ . These were the results of fits to data T. Ferbel had available and were good fits between  $0.2 < x < 0.6$ .

We have tried to reproduce the summer study results. For muons from pion parents and for 400 Gev incident protons we succeed in repeating the number of muons calculated to within 35% of Ferbel's number. For Kaon parents we come closer and get to within 6%. When we do the calculations for an incident energy of 1000 Gev and take the ratio to our numbers for 400 Gev incident energy, we get a ratio of 52. This number compares well to the number 60 quoted in the summer study report. This ratio is for muons with energy above 200 Gev and does not include the increase due to the decrease in the multiple scattering angle. Our calculation is further discussed in Appendix 1.

The summer study report quotes some measured values near the M3 beam for muon fluxes at 400 Gev and 300 Gev primary proton energies. These and the calculated numbers agreed fairly well (a factor of two). It is pointed out in the report that 4-10 feet of steel lowered measured rates by an order of magnitude.

#### Remarks on Production Models

The Stefanski-White production model (Ref. 2) has often been employed in Neutrino Department shielding studies and has been incorporated into a local version (Ref. 3) of the CERN program "HALO". It can be expressed for  $\pi^+$  production by 400 Gev protons as

$$\frac{d\sigma}{dp} (\text{STEF-WHITE}, \pi^+) = 0.32 e^{-8x} \text{ mb}$$

where

$$x = \frac{p}{p_{\max}}$$

(see Appendix 2). The Ferbel 1976 S.S. production formula is

$$\frac{d\sigma}{dx} (\text{FERBEL}, \pi^+) = 1.56 e^{-11x}$$

The  $x$  dependence of the two models is quite different. Using the Stefanski-White expression the ratio of  $\mu^+$  production by 1000 Gev protons to  $\mu^+$  production by 400 Gev protons for  $E(\mu^+) > 200$  Gev, is 17. This is much less than the equivalent number of 43 from the Ferbel model.

The comparison of these two, differing results leads to concern regarding an appropriate production model. Exploration of the question of what is the proper production model has been left out of the purview of this study. Between the Ferbel model and the Stefanski-White model it would be more conservative, when studying muon shielding, to use the Ferbel model--since it gives a higher  $\mu^+$  prediction for 1000 Gev; however, this study has not been consistent in this usage.

#### Use of "HALO" to calculate muon fluxes

The CERN program "HALO" has been utilized to study muon fluxes in the Meson experimental area. This has been done with a succession of better and better approximations to the Meson area magnetic fields and passive steel and dirt shielding (see Fig. 1), for the case of the M-Center target that feeds the M1/M2/M3/M4 beamlines. The Stefanski-White production model has been used for the studies discussed in this section. Both 400 Gev and 1000 Gev were used as incident proton energies. The program was modified to take into account a vertical production angle of 0.6 milli-radian for the M3 beam -- for the 400 Gev case. "HALO" has also been used to cross-check against the Ferbel results and these cross-checks are described in Appendix 3.

The Meson Area was first modelled for "HALO" without any magnetic fields present. The rates calculated near the M3 beam axis were high when compared with fluxes measured by the E533 group (see discussion in Appendix 4). Inclusion of magnetic fields in the calculation necessitated the generation of "HALO"-compatible magnetic field maps for the magnet of interest. We chose to do this on the Fermilab CDC Cyber 175 computers (Ref. 4). The magnets inserted were the first bend magnets in the M2 beam. These serve also as the first magnetic sweepers in the M3 line. The bend consists of 30 feet of B 2-type main ring bending magnets. The magnetic field is 18.5 kilogauss (25 mr bend for a 200 Gev particle). The  $z$  location starts at 236 feet. More details are given in Appendix 5.

With the M2/M3 magnets in place the resulting muon radiation pattern at  $z=1400$  feet is shown in Figure 2. In this figure an entry of "1" represents a bin with a positive muon flux of  $8.7 \times 10^{*4} \mu^+$  per square meter. These results correspond to  $10^{*12}$  400 Gev protons interacting in a "thin" target. The flux represented by a "1" entry in a bin in this figure corresponds to a dosage rate of 0.09 mr/hr (Ref. 5). Indicated on Fig. 2 is an area with the boundaries  $x -420$  to  $-300$  inches,  $y -20$  to  $-4$  inches. This area is centered in  $y$  on the intersection of the proton beam axis with the  $x,y$  plane shown (intersection at  $-10''$ ). The average number of entries per bin in this area is 2.7; the corresponding dosage rate is 0.25 mr/hr (12 sec. cycle time).

For 1000 Gev protons (at 0 mr production angle) the muon radiation pattern at  $z=1400'$  is shown in Figure 3. In this case "1" represents a bin with flux  $1.4 \times 10^{*6} \mu^+ m^{-2}$  -- or 0.3 mr/hr (accelerator cycle is taken to be 60 sec). As before the normalization is  $10^{*12}$  interacting protons. The area indicated on Fig. 3 has boundaries  $x -280$  to  $-180$  inches and  $y -8$  to  $+8$  inches. The average number of entries per bin in this area is 4.7; the corresponding dosage rate is 1.4 mr/hr. This represents an increase of a factor of 6 in going from 400 Gev to 1000 Gev. It includes a factor of 1/5 due to the longer accelerator cycle. A production model with a steeper  $x$  dependence (such as that of the 1976 Ferbel S.S.) would make this ratio higher than 6.

### Muon Measurements

Muon measurements have been made to compare with the "HALO" calculations. These are described in detail in Appendix 6 and the results are shown in Figure 4. The peak rate observed during these measurements was 0.08 mr/hr. The M3 production angles during the measurement were 0.46 mr horizontal and 0.9 mr vertical. The measurements were made at the nominal beam height of 48" above the floor of the Detector building (Ref. 6). Both the measurements and the calculation show the muon rates to be highest between the M2 and M3 beam lines. This is due to the deflection of positive muons in the M2 first bend towards the East. Negative muons are produced at a lower rate (due to the lower  $\pi^-$  production rate) and are deflected in the opposite direction. The rates measured on the west side of the M3 beam are primarily due to negative muons.

### Conclusions

"HALO" calculations of muon fluxes due to proton interactions in the Meson center target give results which agree with measurement to within a factor of 3.1. The calculated rates due to  $\pi^+ \rightarrow \mu^+$  in Figure 2 are actually higher than the measurements discussed in Appendix 6. This could be due to the fact that the second bend string in the M2 line has not been included and probably spreads the distribution of muons out further (see Appendix 6). Other

inadequacies in the model of the shielding probably have smaller effects.

Muon rates calculated with "HALO" runs at 1000 Gev incident energy are a factor of 6 higher than those for 400 Gev incident, when the Stefanski-White production model is used. The calculated 1000 Gev/400 Gev ratio would probably be an additional factor of 4 higher than this if we had used the production model from the Ferbel 1976 summer study.

If we take our calculation for 1000 Gev primary protons for  $\mu^+$  due to  $\pi^+$  decay and multiply by a safety factor of 2 for the contribution due to kaons, direct production (Ref. 7), and negative muons and a safety factor of 4 for differing x dependences of the production models, we then have a maximum muon flux of  $53 \times 10^{+6}$  per square meter for  $10^{+12}$  interacting protons--a dosage rate of 11 mr/hr for a 60 second cycle time. This many interacting protons represents  $1.8 \times 10^{+12}$  protons incident on a 16 inch beryllium target (Ref. 8).

The result that we have just quoted neglects the discrepancy between the calculation and the measurement, however. Recognizing this, we could take our calculated rate of 1.4 mr/hr for 1000 Gev incident and  $10^{+12}$  interacting protons, reduce it by 1/3.1 to account for the discrepancy, boost it by the safety factor of 4 for differing x dependences of the production models, and wind up with a dosage rate of 1.8 mr/hr ( $8.4 \times 10^{+6} \mu \text{ m}^{-2} \text{ pulse}^{-1}$ ). Our range in the prediction for maximum muon dosage rates is, then, from 1.8 to 11 mr/hr when  $1.8 \times 10^{+12}$ , 1000 Gev protons are incident on a 16 inch Be target every 60 sec.

## Appendix 1

Attempt to reproduce Ferbel 1976 S.S. results

For pions the production model used was

$$\frac{d\sigma}{dx} (\pi^-) = 250 e^{-11x} \text{ mb}$$

This gives

$$\frac{d\sigma}{dp} (\pi^+) = \frac{(2.5)(250)}{400} e^{-11x} = 1.562 e^{-11x}$$

The survival fraction for muons with energy above 200 Gev coming from pions produced by 400 Gev protons is

$$\frac{E_\pi - 200}{E_\pi - .57 E_\pi} \left( \frac{\mu \text{ energy range accepted}}{\mu \text{ energy range produced}} \right)$$

as long as  $.57 E_\pi < 200$ . This denominator is correct for the range  $0.5 < X_\pi < 0.8$ , which is the range used in the Ferbel summer study.

The fraction of  $\pi^+$ 's decaying in the first five meters is

$$\left\{ 1 - e^{-5/\gamma c\tau} \right\} \approx \frac{5}{\gamma c\tau} \left( = \frac{.08944}{E_\pi} \right)$$

(where  $\gamma c\tau \approx 56$  meters for a 1 Gev  $\pi^-$ ). The relevant cross section is then

$$\sigma_T \equiv \int_{200}^{320} \left\{ 1.562 e^{-11x/400} \right\} \left\{ \frac{E_\pi - 200}{.43 E_\pi} \right\} \left\{ \frac{.08944}{E_\pi} \right\}$$

$$\sigma_T = 2.36 \cdot 10^{-5} \text{ mb}$$

Since Ferbel calculates the effect of re-absorption in the target, we write

$$\sigma_{\text{EFF}} \equiv \frac{\int_0^L e^{-z/\lambda_p} \sigma_T' e^{-(L-z)/\lambda_\pi} n dz}{\int_0^L e^{-z/\lambda_p} e^{-(L-z)/\lambda_\pi} n dz}$$

where  $L = 20 \text{ cm}$  and  $n = \# \text{ nuclei cm}^{-3}$  in the target.  
Continuing

$$\lambda_p = \frac{1}{\sigma_p n} = \left[ 38.5 (9.01)^{.719} 10^{-27} \frac{6.022}{9.01} 1.85 \cdot 10^{23} \right]^{-1}$$

$$= 43.2 \text{ cm}$$

$$\lambda_p = \left[ 26.9 (9.01)^{.762} 10^{-27} \frac{6.022}{9.01} 1.85 \cdot 10^{23} \right]^{-1}$$

$$= 56.3 \text{ cm}$$

$$\sigma_T' = \sigma_T (9.01)^{0.6666} = 1.02 \cdot 10^{-4} \text{ mb}$$

$$\sigma_{\text{EFF}} = \frac{-\lambda_p \lambda_\pi}{L(\lambda_\pi - \lambda_p)} \left[ e^{-L/\lambda_p} - e^{-L/\lambda_\pi} \right] \sigma_T'$$



$$\sigma_{\text{EFF}} = .66 \sigma_T'$$

The rate per incident proton is then

$$\begin{aligned} R &\equiv \sigma_{\text{EFF}} n L \\ &= (.66) (1.02 \cdot 10^{-4} \cdot 10^{-27}) (1.236 \cdot 10^{23}) (20) \\ &= 1.66 \cdot 10^{-7} \end{aligned}$$

Multiplying by  $3 \times 10^{12}$  protons we have the result of  $5.0 \times 10^{+5} \mu^+$  with energy  $> 200$  Gev per pulse. Since

$$\frac{d\sigma}{dx} (\pi^-) = \frac{1}{2.5} \frac{d\sigma}{dx} (\pi^+)$$

we have for the sum of both signs  $7.0 \times 10^{+5} \mu^+$ . Ferbel quotes  $0.52 \times 10^{+6}$  muons with energy  $> 200$  Gev, and this is the level to which we reproduce his numbers.

A similar calculation for Kaon parents gave a result of  $2.16 \times 10^{+5}$  muons ( $E_p > 200$  Gev). The corresponding summer study number was  $2.3 \times 10^{+5}$  muons; the agreement is good to within 6%.

Rates for 1000 Gev incident protons were calculated in a similar manner and were a factor of 52 higher than the 400 Gev number for muons with  $E_p > 200$  Gev. The corresponding number from the summer study was 60.

## Appendix 2

The Stefanski-White Model

The Stefanski-White production model (Ref 2) gives the formula

$$\frac{d^2N}{dp d\cos\theta} = A B C^2 p^2 \left[ \exp(-8\chi - Cp \sin\theta) \right] \frac{1}{10E_0}$$

where, for  $\pi^+$  production,

$E_0$  = incident energy

$$\chi = p/E$$

$$C = C_0 - 1.43 \exp(\chi - \frac{2}{3}\chi^2)$$

$$C_0 = 6$$

$$A = 5$$

$$B = 8$$

If we integrate over an angular range 0 to  $\theta_m$ , with  $\sin\theta_m \approx \theta_m$ , then

$$\frac{dN}{dp} = \frac{A \cdot B}{10E_0} \left[ \exp(-B\chi) \right] \left[ 1 - (1 + Cp\theta_m) \exp(-Cp\theta_m) \right]$$

For  $E_0 = 400$ ,  $\sigma_{inelastic} \approx 32$  mb, and  $\theta_m = .01$  radians

$$\frac{d\sigma}{dp} = .32 \left[ \exp(-8\chi) \right] g(p)$$

where

$$g(p) = \left[ 1 - (1 + .01 Cp) \exp(-.01 Cp) \right]$$

and  $g(p)$  ranges from 0.997 to 0.99978985 for  $p$  ranging from  $p = 200$  to  $p = 360$ . Therefore

$$\frac{d\sigma}{dp}(\text{STEF-WHITE}, \pi^+) = .32 e^{-8x}$$

where

$$x = \frac{p}{p_{\max}}$$

The values from this expression are plotted in Fig. 5, along with the 1976 S.S. expression and the fit of Wang (Ref. 9). Figure 6 gives the equivalent results for 1000 Gev incident protons.

## Appendix 3

Cross-Check of Calculations

## Test no. 1

"HALO" was run with the Stefanski-White production model for and a 5 meter decay path. The number of muons whose energy exceeded 200 Gev was calculated (for 400 Gev protons on target). For  $10^{12}$  interacting protons the result was  $1.01 \times 10^6 \mu^+$  with  $E > 200$  Gev. A direct integration gave  $1.0 \times 10^6 \mu^+$  and the two results agree to better than the statistical accuracy in the Monte Carlo result.

## Test no. 2

"HALO" was run as for test no. 1, except that the incident energy was 1000 Gev. The decay path was again 5 meters. The accepted x range for the  $\pi^+$  particles was 0.2 to 0.8. The result was  $1.76 \times 10^7 \mu^+$  with  $E_{\mu^+} > 200$  Gev. A direct integration gave  $1.71 \times 10^7 \mu^+$  and the agreement is acceptable.

## Test no. 3

A production model utilizing the Ferbel fit for  $\pi^+$  production was inserted into "HALO" (Ref 1). When run as in test no. 1 the number of  $\mu^+$  with  $E > 200$  Gev was  $7.5 \times 10^5$  for  $10^{12}$  interacting protons. Direct calculation gave  $7.4 \times 10^5 \mu^+$ . The level of agreement is acceptable.

## Test no. 4

We attempted a comparison of a "HALO" run and the Ferbel S.S. calculation. "HALO" was run with the production formula from test No. 3. The energy ranges were  $\pi^+$  200 to 320 Gev,  $\mu^+$  from 200 to 320 Gev. We put in 8.7 meters of steel from 16.4' to 45' to represent target load collimators, 38 meters of steel from 145' to 269' to represent magnets, and 317 meters of dirt (1041') from 269' to 1310' to represent the berm shielding. The muon patterns were examined at  $z = 1400'$ . These absorbers and a fixed  $dE/dz$  (no relativistic rise) gave a fixed energy loss of 200 Gev for all muons reaching  $z = 1400'$ . The angular range of the  $\pi^+$  parents was kept to 0 to 0.2 mr, so that the spread at the end was due only to multiple scattering. We multiplied the resulting number of muons by a factor of 60 to account for the missing pion parents at larger angles (This factor came from comparing this run with 0 to 0.2 mr with another that had 0 to 10 mr  $\pi^+$  production angular range).

The "HALO" result is 280  $\mu^+$  in a region  $1.8 \times 1.8 \text{ m}^2$  centered on the  $O^0$  beam. The number of interacting protons was  $10^{12}$ ; 2000  $\pi^+ \rightarrow \mu^+$  decays were forced to occur in this run. Therefore the fraction of muons falling within a  $3 \text{ m}^2$  circle at  $z = 1400'$  is approximately

$$\frac{280}{2000} \cdot \frac{3.0}{3.24} = 13\frac{1}{2}$$

The Ferbel S.S. calculated 60% as the fraction of muons in a central 3 m\*\*2 area. We attempt an explanation of the discrepancy later.

From the "HALO" result the central dosage rate due to  $\mu^+$  from  $\pi^+$  would be 0.052 mrem/hr. To this we apply a factor of 2 to account for  $\pi^-$ ,  $K^\pm$  parents and a factor of 0.66 to account for absorption in the 20 cm target, and the result is then 0.069 mrem/hr. The equivalent S.S. number is 0.21 mrem/hr (for 10\*\*12 interacting protons). The latter can be multiplied by 0.13/0.60 to account for the difference in the multiple scattering and this would give 0.046 mrem/hr. The level of agreement between the "HALO" result and the corrected S.S. result is a factor of 1.5.

The Ferbel S.S. multiple scattering calculation has a smaller  $y(r.m.s.)$  at  $z = 1400'$  than that in the "HALO" calculation because it does not appear to include the effect of the energy loss of the muons. A multiple scattering calculation was done with (Ref. 10) and without energy loss and the difference between the results of the two calculations can account for the difference between the "HALO" calculation and the S.S. calculation regarding the number of muons falling within the central 3 m\*\*2 circle.

## Appendix 4

Halo Calculations and Counter Rates in Experiments

"HALO" calculations were first done for the M-center target and the M3 line without the presence of magnetic fields. A model was made for the M3 line for the situation that existed before the "Mesopause" (the Meson area shutdown from September, 1978 to June, 1979) and for the situation that existed after the "Mesopause". A "HALO" run for the pre-"Mesopause" conditions gave fluxes of  $1.3 \times 10^{+6} \mu^+$  per square meter from  $\pi^+$  decay per  $10^{+12}$  protons interacting, for the central 1 m x 1 m just outside a beam zone of 16 by 8 square inches. It gave a flux of  $1.7 \times 10^{+5} \mu^+$  for the 1 m by 1 m area just below the central 1 m by 1 m. These calculated rates were high compared to observed fluxes of charged particles near the M3 beam (Ref. 7). The 1976 Ferbel Summer Study quotes measured rates near the M3 beam as ranging between  $0.6 \times 10^{+5}$  to  $2.7 \times 10^{+5}$  muons for  $3 \times 10^{+12}$  protons incident on a 8 inch Be target. The conditions are not described, but if they are similar to those of his calculation the area involved would have been within a 4 mr cone about the beam.

The E533 group (Ref. 12) quotes 350000 charged particles per  $1.5 \times 10^{+12}$  protons in an area 50 x 30 square inches, whose lower edge is 8" above the beam. With the beam stop in place this number dropped to 20000. Both are "post-Mesopause" observations and are rates observed with a 16 inch beryllium primary target. The beam stop is made of permanently magnetized material and is a rectangular block 12' long, 4" wide, and 4" high. It is located at  $z \sim 340$  feet. E533 measured rates of 50000 per spill in the same area before the "Mesopause".

Figure 7 shows the  $\mu^+$  distribution for the "pre-pause" "HALO" calculation. The normalization factor is 15403 muons per unit for  $10^{+12}$  interacting protons. On this figure the M3 beam axis is at  $x=0$ ,  $y=-11.76$  inches. In a 50 by 30 square inch area, whose lower edge is 8" above the beam, we find  $(30)(15403) \mu^+$  on this figure. This converts to 295000 muons for  $1.5 \times 10^{+12}$  protons incident on a 8 inch beryllium target and we see that the number is high compared to the E533 observations. A number more in agreement with their observed rates is gotten by using the output of the "HALO" calculation which includes the effect of 30' of magnet that serves as the M2 first bend and the M3 first magnetic sweeper.

Two further comments are in order. The E533 counters whose rate is being quoted were located about 100 feet downstream of the large aperture 100D40 bending magnet in their experiment. In addition, during the Meson area shutdown, the M3 vacuum pipe from  $z = 1182'$  to  $1312'$  was enlarged from 14" to 36" in diameter and the beam stop was rebuilt to be permanently magnetized.

## Appendix 5

More Detail on the "HALO" Runs

The calculation of the muon fluxes for 400 Gev protons striking the M3 target is described here in more detail than in the main text. Limitations imposed by the "HALO" program will be pointed out as we progress.

The production model employed is the Stefanski-White model. Muons from  $\pi^+$  decay are followed to see if they have sufficient energy to reach the end of the Meson Area and, if so, they are entered into appropriate histograms. The size of the production target is taken to be 0.03 inch by 0.03 inch. Look-up tables are formed for the integrated  $\pi^+$  production formula (see Ref. 1); these are in steps of 10 Gev/c for momenta between 90 and 400 Gev/c and in steps of 0.4 mr for angles between 0 and 5 milliradian. Next, these tables are modified to account for the fact that we choose to force the decay to occur between  $z = -5$  and 173 feet (see Ref. 1). Figure 8 shows the resulting distribution for the  $z$  co-ordinate at which decay of the  $\pi^+$  occurs. Entries into the histogram in Fig. 8 are also subjected to the conditions that the pion stayed within apertures before decaying and that the decay muon had sufficient energy to reach  $z = 1400$  feet. Fig. 9 shows a histogram of  $dN/d\theta$  for pions at  $z = 0$  for  $190 < p < 200$  Gev/c. Fig. 10 shows a scatter plot of  $p$  vs  $\theta$  at  $z = 0$ . Both Figs. 9 and 10 are for only those pions whose decay muons reach the end of the system.

The Meson train-load collimators start 3.3 feet from the target and extend to 50 feet from the target. In the "HALO" input deck these collimators are simulated by 35 collimator elements. This simulation accounts for the tapered apertures -- which go from  $\pm 0.071$  by  $\pm 0.054$  inches square to  $\pm 0.354$  by  $\pm 0.234$  inches square (for the M2/M3 beam).

The region  $z = 45'$  to  $z = 269'$  is the Meson Front End hall (see Fig. 1). For this region the "HALO" data deck has aluminum vacuum pipe to 173', has 30' of M2 quadrupole steel represented by steel 13" by 17" (with a 3" dia hole in the center), and has 30' of M2 bend represented by a main ring B2 magnet field map -- with a central field of 18.54 kg. (The M2 benders have not been offset in the data deck to represent their positioning so as to allow aperture for both the M2 and M3 beams).

From  $z = 269'$  to 347' is the FE hall extension. Further downstream are M3 vacuum pipes and enclosures. Berm vacuum pipe 12" in diameter runs between  $z = 415'$  and 641' and  $z = 695'$  to 1003'. A pipe 36" in diameter runs between  $z = 1055'$  and  $z = 1310'$ . The M3 enclosures are put in as shielding voids, in the shape of simple rectangular boxes. Inside the enclosures we put 6' of steel centered at  $z = 350'$ , 8' of steel centered at  $z = 659'$ , and 9' of steel centered at  $z = 674'$ . The outside dimensions of this steel ranges

from 12 by 12 square inches at  $z = 350'$  to 36 by 36 square inches at  $z = 674'$ . There is a central hole in the steel which ranges from 4 by 2.4 square inches to 6.6 by 4 square inches and is meant to roughly match the M3 beam acceptance.

The dirt berm surrounding the enclosures and berm vacuum pipes has an actual topography which is complex compared to its possible representation by "HALO" shielding configurations. Fig. 11 shows rough contour lines at its top and at its toe. This figure also shows the slope of the trajectory of the M1 and M6 beam lines and it is not surprising that the slope of the toe contour is approximately the same. From this figure we have made rectangular approximations of the dirt berm for use in "HALO". The "tunnel" feature of "HALO" has been used to account for the presence of the dirt berm. From  $z = 1055'$  to  $z = 1310'$  the outside dimensions of this dirt tunnel in the input deck are 168' horizontally and 20' vertically (both centered on the M3 beam). From  $z = 1310'$  to  $z = 1372'$  the horizontal size of the dirt tunnel is increased to 192'.

Changes made to "HALO" by A. Malensk for his studies of muon flux at the 15' bubble chamber were borrowed, in part. These changes modernized the decay constants and radiation lengths (Ref. 12), put in the Stefanski-White production model, included the "density" effect for collision energy losses and pair production in the  $dE/dz$  for muons in iron and dirt. Tables 1 and 2 summarize the changes to decay constants and radiation lengths. The  $dE/dz$  expressions for iron and soil are give in Table 3. These give values that are reasonable matches to the  $dE/dz$  values in Figure 3 of TM-786, "Muon  $dE/dz$  and Range Tables for Tevatron Energies: Results for some Shielding Materials", by G. Koizumi.

It is possible to question the simplicity of the shielding model used in these "HALO" studies. This simplicity is imposed by the restrictions inherent in using "HALO". "HALO" is meant to treat a case of one target feeding one beam which travels down one tunnel. We also note here that the magnetic field of the M3 sweeping magnets at  $z = 391'$  and  $675'$  is not included (these have a polarity opposite to that of the M2 bend at  $z = 247'$ ).

The M2 benders centered at  $z = 374.5'$  and  $z = 391'$  are main ring B2-type magnets and total 30' in length. They have outside dimensions 25.25 by 14.25 square inches. The effect of their magnetic field has not been included. The muon distribution pattern at  $z = 352'$  shown in Fig. 13 suggests that the magnetic field of these magnets should have a quite noticeable effect -- since many of the muons making it to the end in our study pass through these magnets. The M3 sweeping magnet centered at  $z = 391'$  would have little effect -- judging by Fig. 13.

A further improvement to the shielding model would be to account for the M2 tunnel from  $z = 1003'$  to  $z = 1123'$ , Judging by Fig. 14, including the full length of this tunnel would have the effect of removing about 70' of dirt where many muons pass through. Part of



this tunnel is accounted for by the inclusion of the M3 tunnel from  $z = 1003'$  to  $z = 1055'$ . The M2 bend magnets in the enclosure from 1003 to 1123 form the third bend point of the M2 beam. Our omission of those magnets should represent a small effect, due to the large vertical size of the muon distribution at that point (see Fig. 14 ). An improved calculation would account for the second M2 bend point and 70 more feet of enclosure at  $z \sim 1100$  feet.

## Appendix 6

Small-Scale Survey of Muon Radiation

A small-scale survey of muon background in the Meson Detector Building was made January 19, 1980 in order to have experimentally measured numbers for comparison with those calculated by "HALO" (Ref. 12 ). The measurements were made between M2 and M3 (4 positions), between M3 and M5 (5 positions), and between M1 and M2 (one position). All were made at the nominal beam height of 48 inches and at a  $z$  value = 1386 feet. The portable muon scintillator telescope described as "system 2" in Table 4 was used (Ref. 13 ).

The instrument was mounted at beam height on a tripod which allowed measurement of relative horizontal and vertical angles. The muon radiation was very directional--as can be seen from figures 15 and 16 . At each transverse ( $x$ ) position the instrument was pointed in the direction of maximum flux and the number of coincidences were recorded for seven beam pulses (the number of protons on target was recorded for the same seven pulses).

The angular widths in Figs. 15 and 16 correspond to the angular cone defined by the two scintillators. This suggests that the muons enter the instrument relatively parallel. Fig. 17 from the "HALO" calculations also shows small angular spreads. We conclude, therefore, that we may take the counts that we observe as the number of muons crossing a 17.8 square centimeter area. By doing so we arrive at the entries in Table 5 .

Column 5 of this table is graphed on Fig. 4 . The horizontal and vertical production angles of the M3 beam at the time of the measurement were 0.46 mr and  $\sim 1$  mr. The proton beam was going downward and was being bent toward the M1 beam.

## REFERENCES

1. Ch. Iselin, CERN 74-17, "Halo--A Computer Program to Calculate Muon Halo", 1974. See Fermilab Computer Library Program document PM-33.
2. FN-292, R.J. Stefanski and H.B. White, "Neutrino Flux Distributions", May 10, 1976
3. The local version originally found on the Cyber 175 had a Sanford-Wang production model built into it. The modification to incorporate the Stefanski-White model is due to A. Malensk. We use here Version 2.2 of "HALO". At CERN the version number has advanced to 2.5.
4. The program "LINDA" is partially described in the book, "Particle Accelerator Design -- Computer Programs", by J. Colonias, Academic Press, 1974, pp. 39-56. The Cyber 175 version was imported from LBL by D. Carey. There is a 370/195 version on the ANL computer, but it was our decision to use the Cyber 175 version in order to "comission" the local "LINDA" capability.
5. Section 12.3.3 of the Fermilab Radiation Guide, 3rd edition, P.J. Gollon, Editor, September, 1978 supplies the number  $7.8 \text{ muons cm}^{-2} \text{ sec}^{-1} = 1 \text{ mrem/hr}$  for muons outside a thick shield. This translates to  $0.94 \times 10^{*6} \text{ muons m}^{-2} \text{ pulse}^{-1}$  for an accelerator with a repetition rate of a pulse every 12 seconds.
6. Since the protons were targetted downward at an angle of 0.9 mr, a height above the floor 15 inches less than the nominal 48 inch beam height would have been a better choice. Figure 2 suggests, however, that the position dependence is not strong enough for 15 inches to make a significant difference.
7. The rate for direct production of muons can be crudely estimated relative to pion decay by using a factor of  $10^{*-4}$  times the pion production rate as the estimate for direct production. The decay fraction for a pion of energy E Gev in L meters is

$$\approx \frac{L}{\gamma c \tau} = \frac{.256}{E} L$$

For a 200 Gev pion the fraction is  $10^{*-4}$  when  $L = 1.1$  meter.

8. For this calculation we use for the beryllium absorption cross section

$$(38.6)(9.01)^{0.719} = 187.5$$

These numbers are taken from the preprint A. S. Carroll, et. al., Fermilab Pub-78/80-EXP, October, 1978 (Submitted to Physics Letters). The resulting absorption length is 43.1 cm and is larger than the value of 36.7 cm given in the Particle Properties Data Booklet, April, 1978.

9. C.L. Wang, Phys. Rev. D 7, 2609 (1973). See also Phys. Rev. D10, 3876 (1974)
10. L. Eyges, Phys. Rev. 74, 1534 (1948).  
This paper was brought to my attention by Fermilab TM-261, "Muon Shielding: Multiple Coulomb Scattering of Muons with Energy Loss", by D. Theriot. The reader of either of these papers is advised to check the equations for an error of a factor of two.
11. The measument equipment is, of course, insensitive to the sign of the muons. A great deal of sign separation occurs at the first bending magnets. The positive muons are mostly bent to the east of the M3 line. They are what has been calculated and they are responsible for the highest points seen in Figure 4 .
12. private communication, Bruce Winstein.
13. The muon measurements were performed in conjunction with W. Baker.
14. The portable scintillator telescope is described in section 4.10 of the Fermilab Radiation Guide, op. cit. B.J. Holt was very helpful in arranging the loan of this instrument.

HALO  
Program  
(Version 2.2)

A. Malensk  
change

Particle  
Data Booklet  
April, 1978

$c \tau$  values (meters)

$\pi$ Decay	7.64	7.8	7.804
K Decay	3.67	3.71	3.709

Branching Ratio

$K \rightarrow \mu \nu$	0.58	0.63	0.635
-------------------------	------	------	-------

Table 1

Change in Decay Constants

Material	Radiation Lengths (meters)		
	HALO Program (Version 2.2)	A. Malensk change	Particle Data Booklet April, 1978
AIR	312.4	312.4	300.5
FE	.018	.0177	.0176
CU	.0147	.0147	.0143
DIRT	.15	.165	
Be	.338	.338	.353
Pb	.0051	.0051	.0056
Al	.0886	.0886	.089

Table 2  
Change in Radiation Lengths

p range	dE/dz for Iron (Gev/meter)
$< 1$	1.16
$1 < p < 100$	$1.26 + 0.12 \ln(p)$
$100 < p < 400$	$7.72 - 2.69 \ln(p) + 0.31 (\ln(p))^2$
$400 < p < 1000$	$32.08 - 10.61 \ln(p) + 0.954 (\ln(p))^2$

dE/dz for Iron

p range	dE/dz for Soil (Gev/meter)
$< 1$	.46
$1 < p < 100$	$0.35 + 0.0287 \ln(p)$
$100 < p < 400$	$1.51 - 0.434 \ln(p) + 0.0466 (\ln(p))^2$
$400 < p < 1000$	$3.3854 - 1.184 \ln(p) + 0.107 (\ln(p))^2$

dE/dz for Soil (Gev/meter)

Table 3

These detectors and the associated electronics can be carried by one person. Their LED scalers can be set to accumulate counts in one of four modes: coincidences between the two detectors, singles in either one of the two detectors, or random (i.e., delayed) coincidences between the front and back detectors.

Scintillator Diameter	4.8 cm
Scintillator Area	17.8 cm <sup>2</sup>
Scintillator Spacing	53 cm
Half-Angle of Cone of Sensitivity	45 mrad (2.6°)

#### Properties of Radiation Physics "Muon Finder"

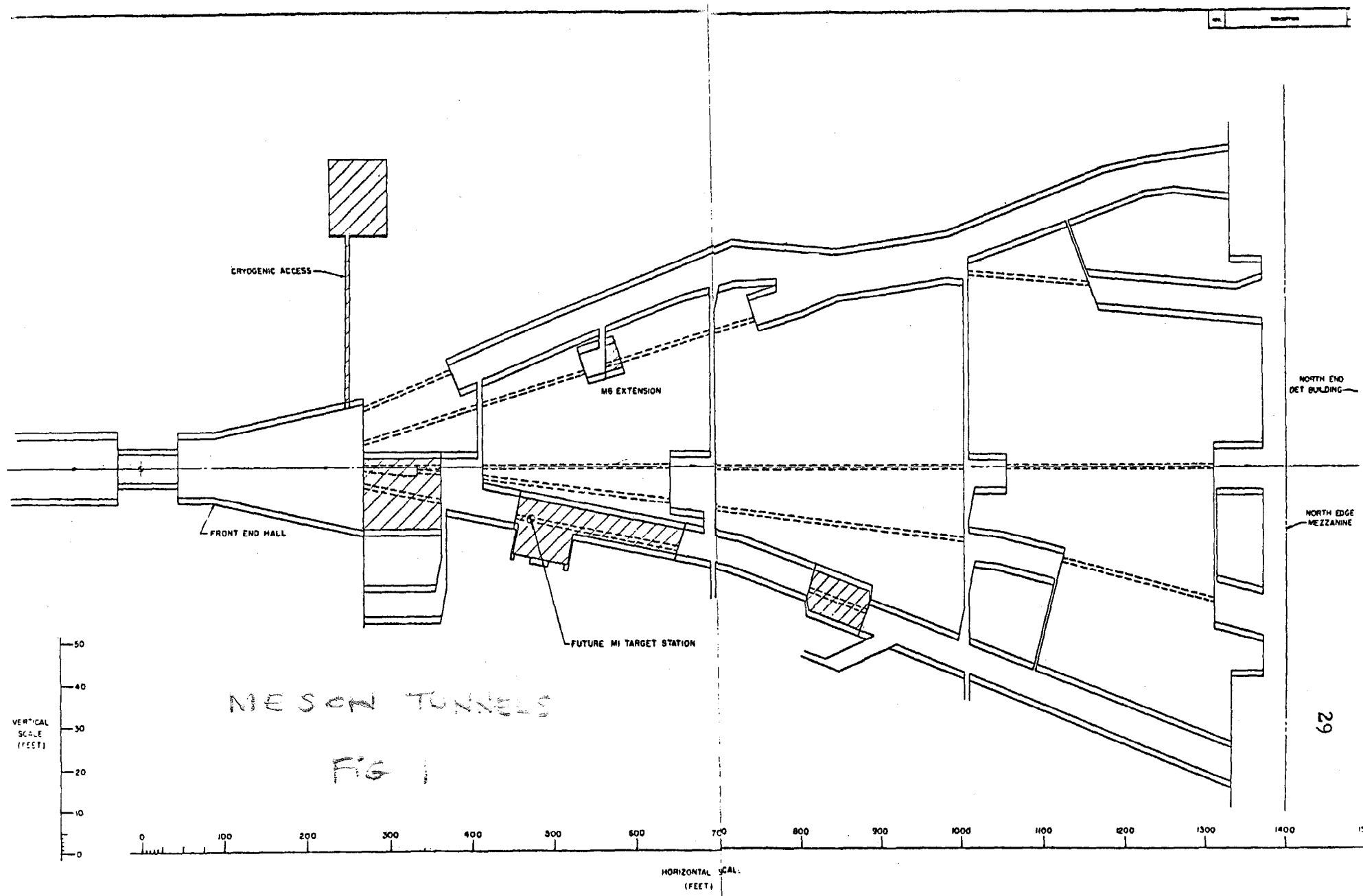
Table 4



x value (inches)	No. of counts	No. of protons $\times 10^{*-12}$	No. of muons $\times 10^{*-12}$ interacting protons	Radiation mrem/hr
-628	75	3.7	1.7	0.018
-296	2423	25.9	7.8	0.084
-234	972	27	3.0	0.032
-177	423	26	1.4	0.015
-124	1014	25	3.4	0.036
123	301	22.3	1.1	0.012
196	254	25.4	0.8	0.009
264	423	24.5	1.4	0.015
325	332	25.7	1.1	0.012
411	95	25	0.3	0.0034

Table 5

Muon Flux Measurements  
at Nominal Beam Height



HISTOGRAM NO. 1  
 HORIZONTAL AXIS... X IN IN FOR HALO AT 1405.000 FT  
 VERTICAL AXIS... Y IN IN FOR HALO AT 1405.000 FT

			-600.00	-400.00	-200.00	- .00	SUMS
-120.000	TO	-116.000	I	1	1	1	3
-116.000	TO	-112.000	I	1	1	1	4
-112.000	TO	-108.000	I	1	1	1	3
-108.000	TO	-104.000	I			1	1
-104.000	TO	-100.000	I	1	2	1	3
-100.000	TO	-96.000	I		2	1	3
-96.000	TO	-92.000	I	1	1	1	5
-92.000	TO	-88.000	I		1	1	4
-88.000	TO	-84.000	I		1	2	3
-84.000	TO	-80.000	I	1	2	2	3
-80.000	TO	-76.000	I	1	1	1	3
-76.000	TO	-72.000	I	1	1	1	3
-72.000	TO	-68.000	I	1	1	1	3
-68.000	TO	-64.000	I	1	1	1	3
-64.000	TO	-60.000	I	1	1	1	3
-60.000	TO	-56.000	I	1	1	1	3
-56.000	TO	-52.000	I	1	1	1	3
-52.000	TO	-48.000	I	1	1	1	3
-48.000	TO	-44.000	I	1	1	1	3
-44.000	TO	-40.000	I	1	1	1	3
-40.000	TO	-36.000	I	1	1	1	3
-36.000	TO	-32.000	I	1	1	1	3
-32.000	TO	-28.000	I	1	1	1	3
-28.000	TO	-24.000	I	1	1	1	3
-24.000	TO	-20.000	I	1	1	1	3
-20.000	TO	-16.000	I	1	1	1	3
-16.000	TO	-12.000	I	1	1	1	3
-12.000	TO	-8.000	I	1	1	1	3
-8.000	TO	-4.000	I	1	1	1	3
-4.000	TO	.000	I	1	1	1	3
.000	TO	4.000	I	1	1	1	3
4.000	TO	8.000	I	1	1	1	3
8.000	TO	12.000	I	1	1	1	3
12.000	TO	16.000	I	1	1	1	3
16.000	TO	20.000	I	1	1	1	3
20.000	TO	24.000	I	1	1	1	3
24.000	TO	28.000	I	1	1	1	3
28.000	TO	32.000	I	1	1	1	3
32.000	TO	36.000	I	1	1	1	3
36.000	TO	40.000	I	1	1	1	3
40.000	TO	44.000	I	1	1	1	3
44.000	TO	48.000	I	1	1	1	3
48.000	TO	52.000	I	1	1	1	3
52.000	TO	56.000	I	1	1	1	3
56.000	TO	60.000	I	1	1	1	3
60.000	TO	64.000	I	1	1	1	3
64.000	TO	68.000	I	1	1	1	3
68.000	TO	72.000	I	1	1	1	3
72.000	TO	76.000	I	1	1	1	3
76.000	TO	80.000	I	1	1	1	3
80.000	TO	84.000	I	1	1	1	3
84.000	TO	88.000	I	1	1	1	3
88.000	TO	92.000	I	1	1	1	3
92.000	TO	96.000	I	1	1	1	3
96.000	TO	100.000	I	1	1	1	3
100.000	TO	104.000	I	1	1	1	3
104.000	TO	108.000	I	1	1	1	3
108.000	TO	112.000	I	1	1	1	3

112.000 TO 116.000 I 111 1 1 I 5  
 116.000 TO 120.000 I 1 I I I 1  
 SUMS  
 123476988877431  
 S 133656423021222463951626768395

UNDER UNDER IN OVER HMEAN = -267.44317 IN  
 IN 0 55 38 VMEAN = 2.0616 IN  
 OVER 1 56 42 CORRELATION = .02401  
 TOTAL NUMBER OF PARTICLES CONSIDERED 1146

MUON DISTRIBUTION  
 400 GEV INCIDENT  
 FIGURE 2

HISTOGRAM NO. 14  
HORIZONTAL AXIS...  
VERTICAL AXIS...

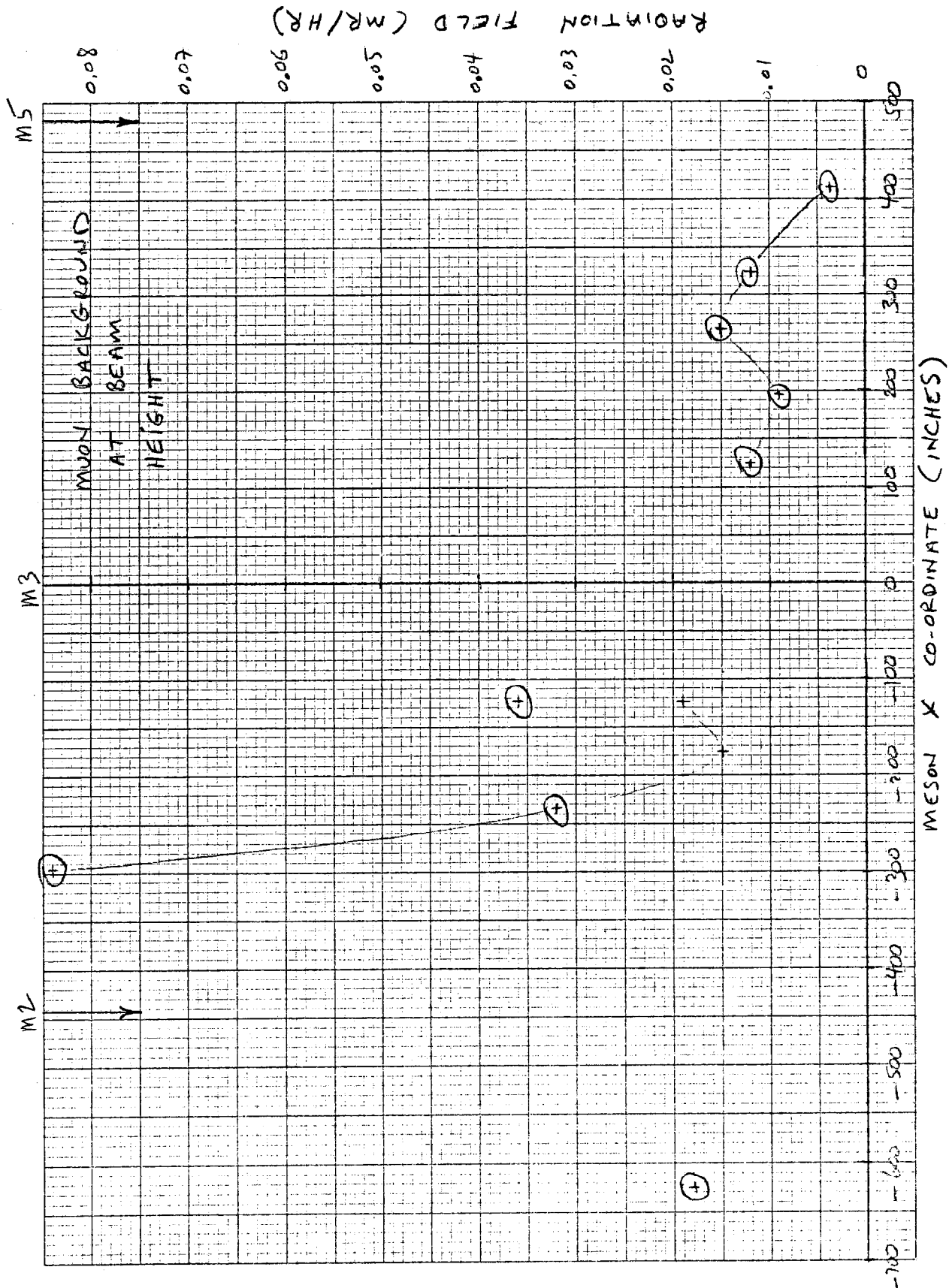
IN IN		FOR HALO AT		DATE 70/12/29	POSITION NO.	
IN IN	FOR HALO AT	1405.000	FT		611	
IN IN	FOR HALO AT	1405.000	FT		612	

TIME 13.54.23.

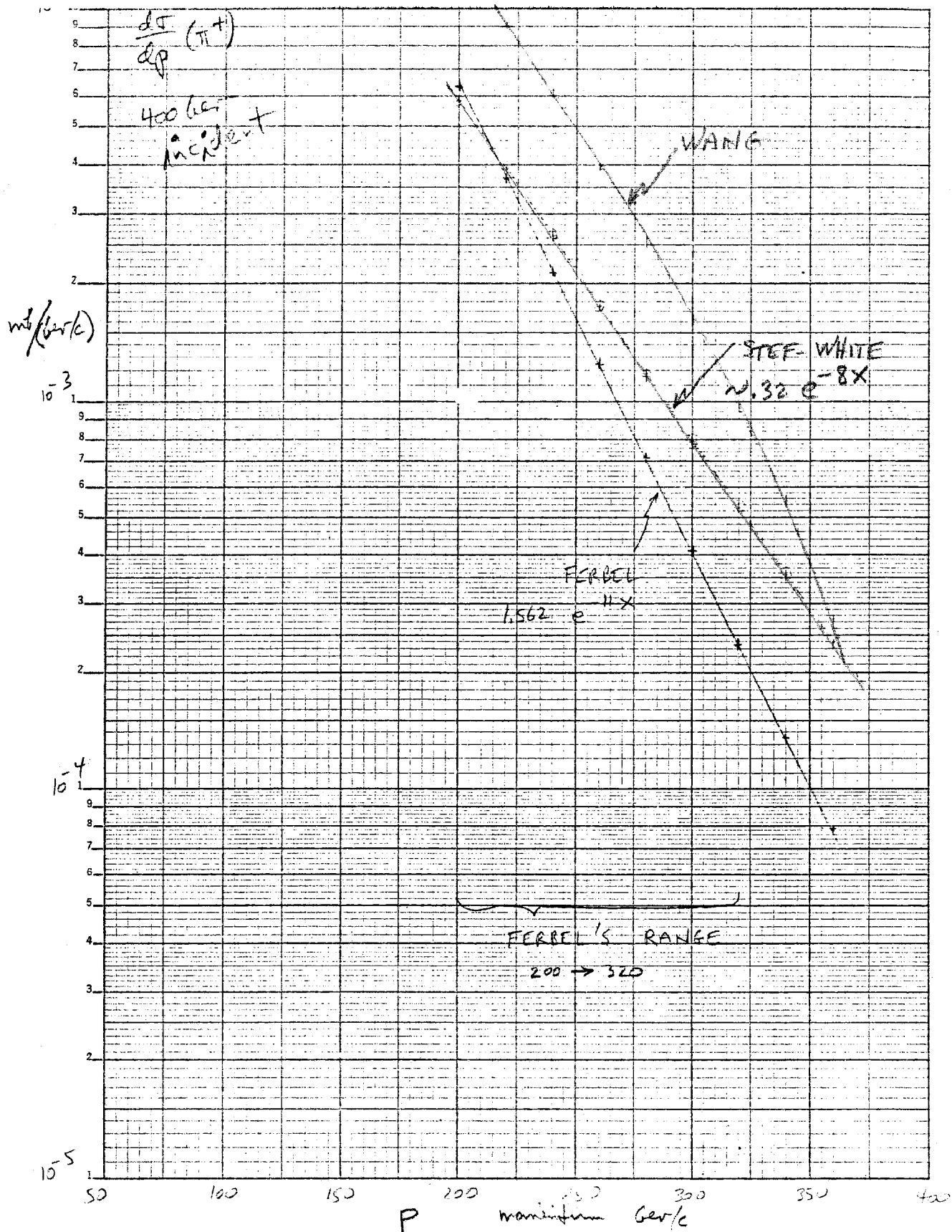
	1440.00	1240.00	1040.00	840.00	640.00	440.00	240.00	40.00	SUM
11.000	11.000								1
12.000	12.000								1
13.000	13.000								1
14.000	14.000								1
15.000	15.000								1
16.000	16.000								1
17.000	17.000								1
18.000	18.000								1
19.000	19.000								1
20.000	20.000								1
21.000	21.000								1
22.000	22.000								1
23.000	23.000								1
24.000	24.000								1
25.000	25.000								1
26.000	26.000								1
27.000	27.000								1
28.000	28.000								1
29.000	29.000								1
30.000	30.000								1
31.000	31.000								1
32.000	32.000								1
33.000	33.000								1
34.000	34.000								1
35.000	35.000								1
36.000	36.000								1
37.000	37.000								1
38.000	38.000								1
39.000	39.000								1
40.000	40.000								1
41.000	41.000								1
42.000	42.000								1
43.000	43.000								1
44.000	44.000								1
45.000	45.000								1
46.000	46.000								1
47.000	47.000								1
48.000	48.000								1
49.000	49.000								1
50.000	50.000								1
51.000	51.000								1
52.000	52.000								1
53.000	53.000								1
54.000	54.000								1
55.000	55.000								1
56.000	56.000								1
57.000	57.000								1
58.000	58.000								1
59.000	59.000								1
60.000	60.000								1
61.000	61.000								1
62.000	62.000								1
63.000	63.000								1
64.000	64.000								1
65.000	65.000								1
66.000	66.000								1
67.000	67.000								1
68.000	68.000								1
69.000	69.000								1
70.000	70.000								1
71.000	71.000								1
72.000	72.000								1
73.000	73.000								1
74.000	74.000								1
75.000	75.000								1

[illegible]

MUON DISTRIBUTION  
1000 GEV INCIDENT  
FIG. 3



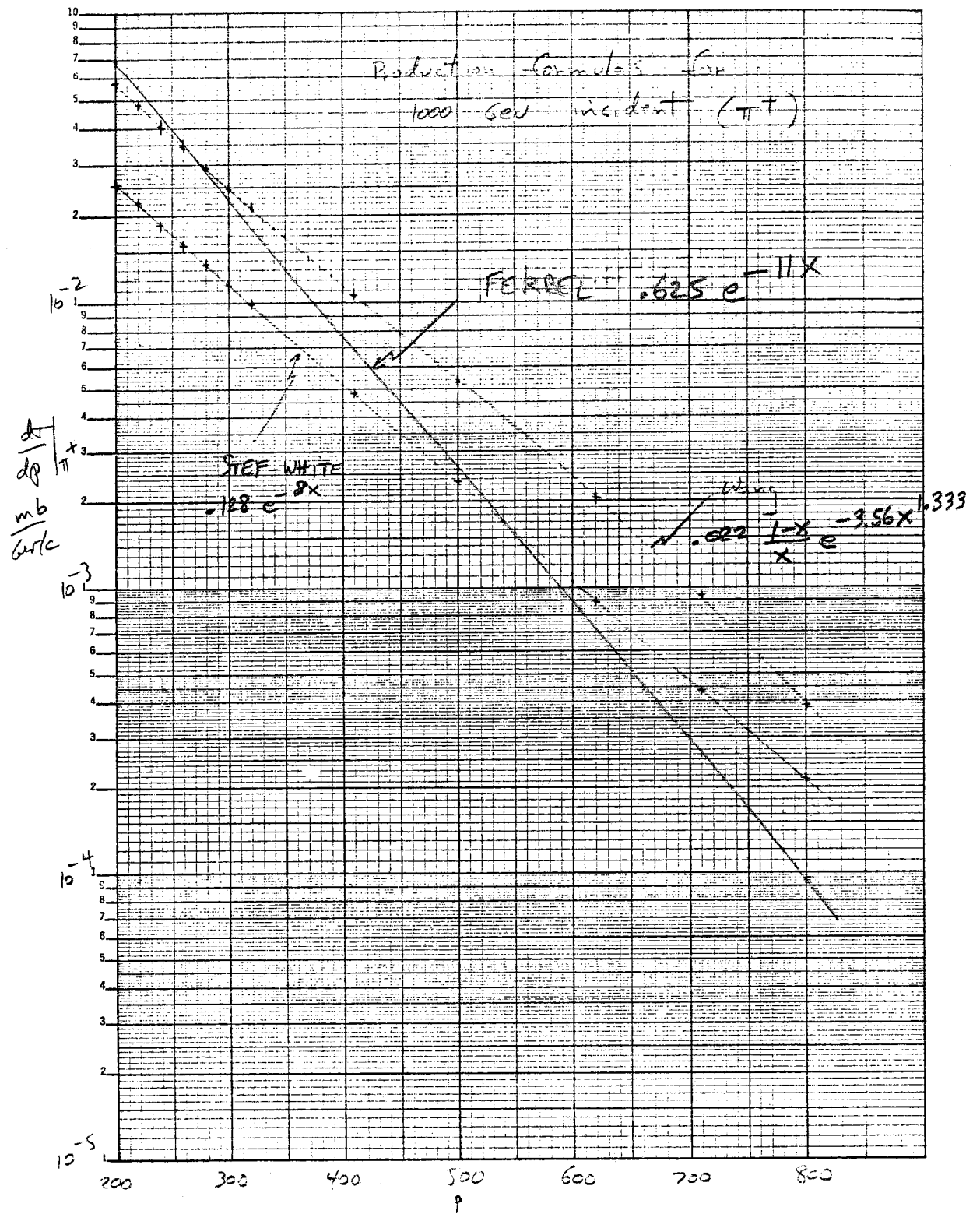
MUON MEASUREMENTS  
FIGURE 4



PRODUCTION CURVE

400 GeV

FIGURE 5

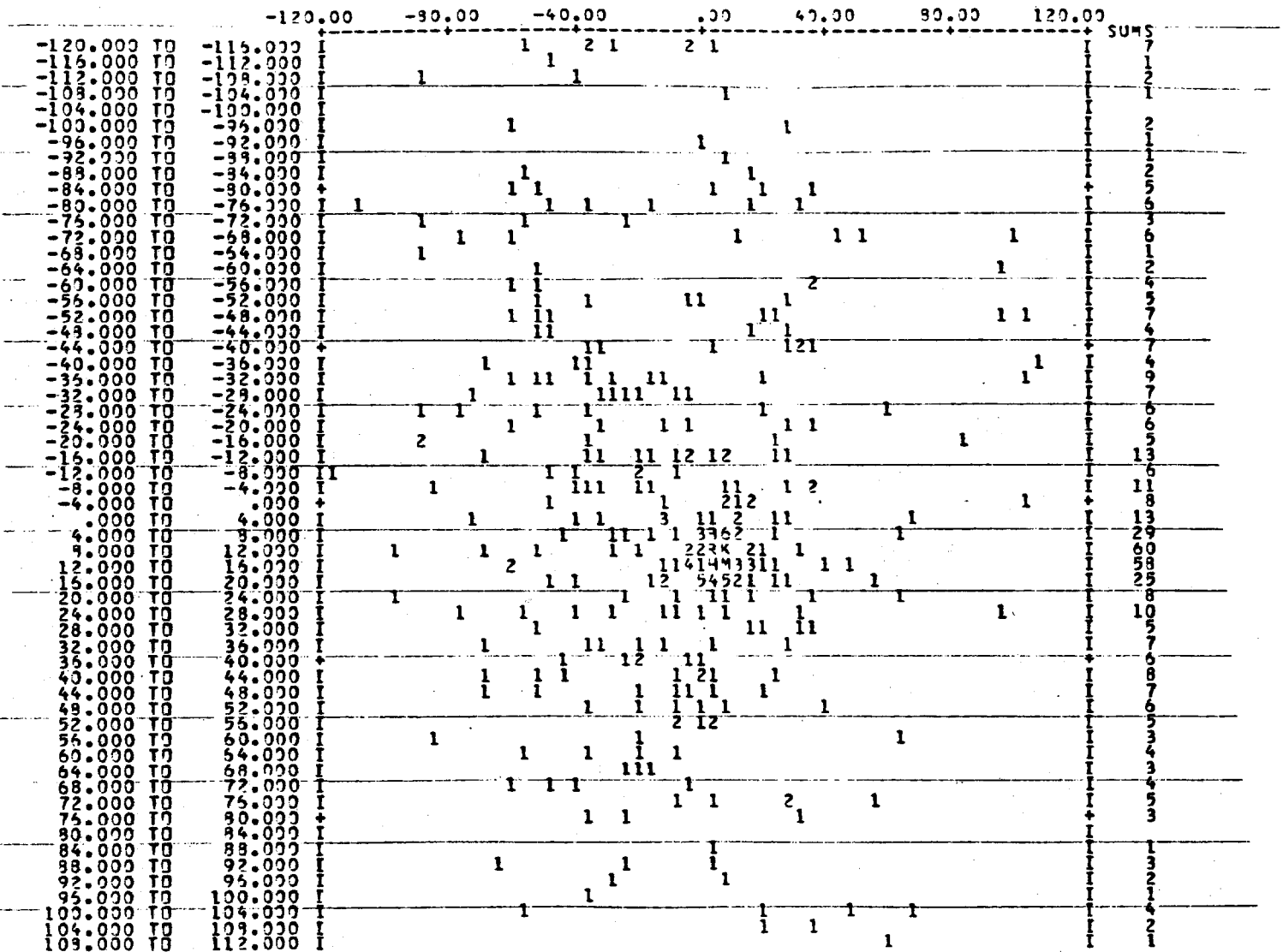


PRODUCTION CURVES

1000 GeV

FIGURE 6

HISTOGRAM NO. 19 DATE 79/05/21. TIME 15.59.25  
 HORIZONTAL AXIS... X IN IN FOR HALO AT 1399.999 FT (POSITION NO. 65)  
 VERTICAL AXIS... Y IN IN FOR HALO AT 1399.999 FT (POSITION NO. 65)





HISTOGRAM NO. 4      Z      IN FT      FOR PI      AT DECAY POSITION      DATE 80/03/05.  
 DISTRIBUTION OF  
 FLAGS = HEND

SCALE FACTOR... 1 X = 10 ENTRIES.

LESS THAN	0.000	0	
0.000 TO	5.000	239	XXXXXXXXXXIXXXXXXXXXXXIXXX9
5.000 TO	10.000	80	XXXXXXXXXX
10.000 TO	15.000	58	XXXXXXXX8
15.000 TO	20.000	47	XXXXX7
20.000 TO	25.000	22	XX2
25.000 TO	30.000	34	XXXX4
30.000 TO	35.000	28	XX8
35.000 TO	40.000	18	X8
40.000 TO	45.000	27	XX7
45.000 TO	50.000	17	X7
50.000 TO	55.000	21	XX1
55.000 TO	60.000	21	XX1
60.000 TO	65.000	25	XX5
65.000 TO	70.000	26	XX6
70.000 TO	75.000	30	XXX
75.000 TO	80.000	27	XX7
80.000 TO	85.000	20	XX
85.000 TO	90.000	25	XX5
90.000 TO	95.000	21	XX1
95.000 TO	100.000	15	X5
100.000 TO	105.000	19	X9
105.000 TO	110.000	25	XX5
110.000 TO	115.000	25	XX5
115.000 TO	120.000	22	XX2
120.000 TO	125.000	11	X1
125.000 TO	130.000	23	XX3
130.000 TO	135.000	25	XX5
135.000 TO	140.000	21	XX1
140.000 TO	145.000	29	XX9
145.000 TO	150.000	27	XX7
150.000 TO	155.000	30	XXX
155.000 TO	160.000	25	XX5
160.000 TO	165.000	19	X9
165.000 TO	170.000	19	X9
170.000 TO	175.000	13	X3
175.000 TO	180.000	12	X2

GREATER THAN 180.000 0

HMEAN = 63.23972 FT R.M.S. HALF WIDTH = 56.92601 FT

TOTAL NUMBER OF PARTICLES CONSIDERED 1146

DECAY POINT DISTRIBUTION

FIG. 8

HISTOGRAM NO. 8 THETA IN MR FOR PI AT DATE 80/03/05.  
 DISTRIBUTION OF HEND 0.000 FT (POSITION)  
 FLAGS = RP

SCALE FACTOR... 1 X = 1 ENTRIES.

LESS THAN 0.000 0

0.000	TO	.200	12	XXXXXXXXXX
.200	TO	.400	26	XXXXXXXXXXXXXXXXXXXXXXXXXX
.400	TO	.600	24	XXXXXXXXXXXXXXXXXXXXXX
.600	TO	.800	5	XXXXX
.800	TO	1.000	4	XXXX
1.000	TO	1.200	3	XXX
1.200	TO	1.400	2	XX
1.400	TO	1.600	1	X
1.600	TO	1.800	1	X
1.800	TO	2.000	1	X
2.000	TO	2.200	2	XX
2.200	TO	2.400	1	X
2.400	TO	2.600	0	
2.600	TO	2.800	1	X
2.800	TO	3.000	0	
3.000	TO	3.200	0	
3.200	TO	3.400	1	X
3.400	TO	3.600	1	X
3.600	TO	3.800	0	
3.800	TO	4.000	0	
4.000	TO	4.200	2	XX
4.200	TO	4.400	1	X
4.400	TO	4.600	0	
4.600	TO	4.800	0	
4.800	TO	5.000	0	
5.000	TO	5.200	0	
5.200	TO	5.400	0	
5.400	TO	5.600	0	
5.600	TO	5.800	0	
5.800	TO	6.000	0	
6.000	TO	6.200	0	
6.200	TO	6.400	0	
6.400	TO	6.600	0	
6.600	TO	6.800	0	
6.800	TO	7.000	0	
7.000	TO	7.200	0	
7.200	TO	7.400	0	
7.400	TO	7.600	0	
7.600	TO	7.800	0	
7.800	TO	8.000	0	
8.000	TO	8.200	0	
8.200	TO	8.400	0	
8.400	TO	8.600	0	
8.600	TO	8.800	0	
8.800	TO	9.000	0	
9.000	TO	9.200	0	
9.200	TO	9.400	0	
9.400	TO	9.600	0	
9.600	TO	9.800	0	
9.800	TO	10.000	0	

GREATER THAN 10.000 0

HMEAN = .78544 MR R.M.S. HALF WIDTH = .91281 MR

TOTAL NUMBER OF PARTICLES CONSIDERED 88

ANGULAR DISTRIBUTION

FIGURE 9

HISTOGRAM NO. 10  
HORIZONTAL AXIS...  
VERTICAL AXIS...  
FLAGS - HEND

P THETA IN GEV/C FOR PI AT  
THETA IN MR FOR PI AT

DATE 90/03/05  
0.000 FT (POSITION)  
0.000 FT (POSITION)

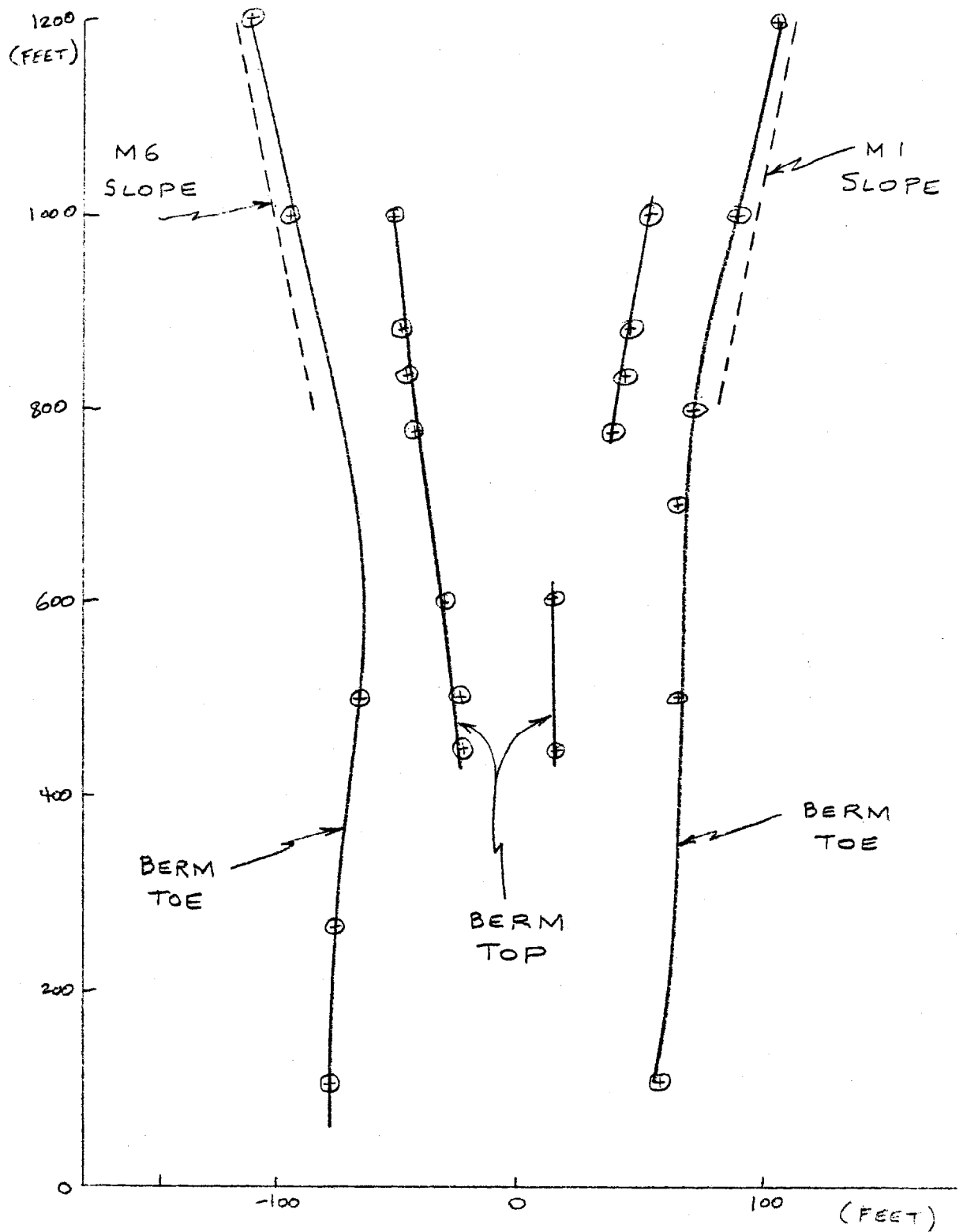
		90.00	190.00	290.00	390.00	SUMS
0.000	TO	.200	I	8098CDA385753532 2	I	119
.200	TO	.400	I 2 1	5LQJYOMNYS IIDA953953222	I 1	341
.400	TO	.600	I 4 6723	SUMTCQUORHG6CA76673423	I 12	366
.600	TO	.800	I 14 2263	746544548751522121	I 2 11	95
.800	TO	1.000	I 11 21	341444 11123 1 121 1	I 1	39
1.000	TO	1.200	I 1121	13221332 1 2 1 1 1	I 1	28
1.200	TO	1.400	I 1	3 2222113 111 1	I 1	21
1.400	TO	1.600	I 1	1 2 2 1 3 1 21 21 1	I 1	18
1.600	TO	1.800	I 1	1 12 21 1111 1	I 1	12
1.800	TO	2.000	I	1 21111 3 1 1	I	12
2.000	TO	2.200	I	21 13 3 2 22 2 1	I	19
2.200	TO	2.400	I	1 1 1 112 111	I	9
2.400	TO	2.600	I	1 1 11 112 1	I	8
2.600	TO	2.800	I 1	1 1 1 1	I	5
2.800	TO	3.000	I 1	1 1 12 1 2	I	8
3.000	TO	3.200	I 1	11 1 11 1	I	7
3.200	TO	3.400	I 1	1 11122 2	I	10
3.400	TO	3.600	I	1 2 1 1	I	4
3.600	TO	3.800	I	1 1 21 1	I	6
3.800	TO	4.000	I	1 1 1 2 1	I	6
4.000	TO	4.200	I	1 1 1 1 1	I	3
4.200	TO	4.400	I	1 1 1 1	I	3
4.400	TO	4.600	I	1 1 1 1	I	3
4.600	TO	4.800	I	11 1 1	I	2
4.800	TO	5.000	I	11	I	
5.000	TO	5.200	I		I	
5.200	TO	5.400	I		I	
5.400	TO	5.600	I		I	
5.600	TO	5.800	I		I	
5.800	TO	6.000	I		I	
6.000	TO	6.200	I		I	
6.200	TO	6.400	I		I	
6.400	TO	6.600	I		I	
6.600	TO	6.800	I		I	
6.800	TO	7.000	I		I	
7.000	TO	7.200	I		I	
7.200	TO	7.400	I		I	
7.400	TO	7.600	I		I	
7.600	TO	7.800	I		I	
7.800	TO	8.000	I		I	
8.000	TO	8.200	I		I	
8.200	TO	8.400	I		I	
8.400	TO	8.600	I		I	
8.600	TO	8.800	I		I	
8.800	TO	9.000	I		I	
9.000	TO	9.200	I		I	
9.200	TO	9.400	I		I	
9.400	TO	9.600	I		I	
9.600	TO	9.800	I		I	
9.800	TO	10.000	I		I	
P, $\theta$ SCATTER CUT						
FIG. 10						
SUMS						
S U						
V1 1112797987877553331121						
S27253590398735696702860887555245						

UNDER IN OVER

UNDER 0 0 0  
IN 0 1146 0  
OVER 0 0 0

HMEAN = 214.42582 GEV/C  
VMEAN = .72067 MR  
CORRELATION = -.14743

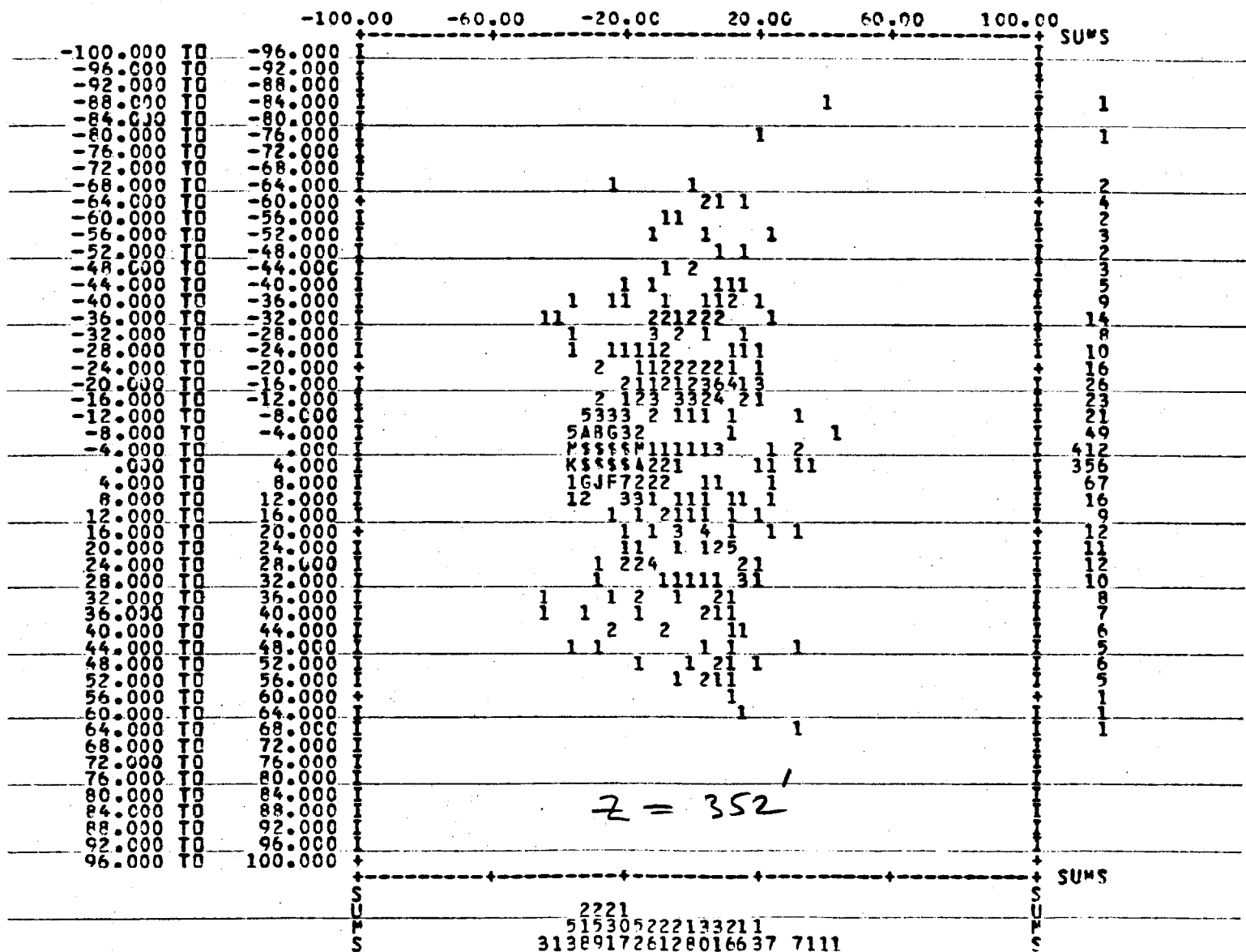
TOTAL NUMBER OF PARTICLES CONSIDERED 1146



BERM. CONTOURS

FIG. 11

HISTOGRAM NO. 11  
 HORIZONTAL AXIS... X IN IN FOR HALO AT 352.000 FT (POSITION NO. 45)  
 VERTICAL AXIS... Y IN IN FOR HALO AT 352.000 FT (POSITION NO. 45)  
 FLAGS \* HEND



UNDER IN OVER

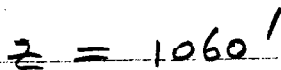
UNDER 0 0 0  
 IN 0 1144 0  
 OVER 0 2 0

HMEAN = -22.69747 IN  
 VMEAN = -4.8791 IN  
 CORRELATION = -.01252

SIGMAH =  
 SIGMAV =

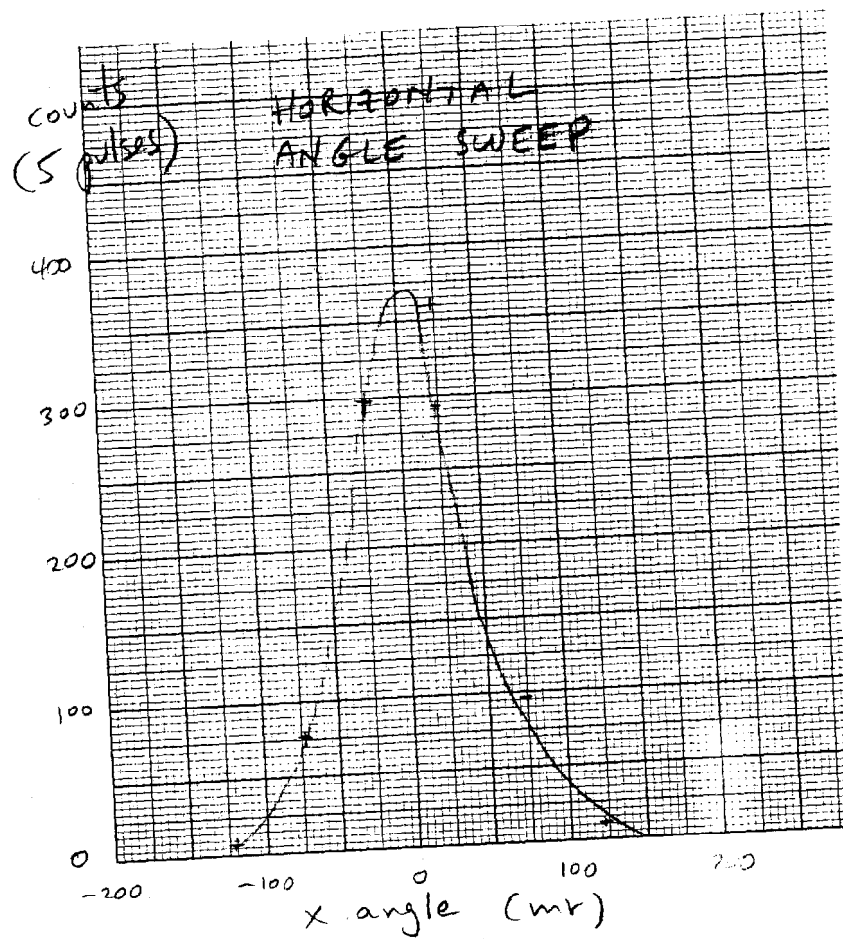
TOTAL NUMBER OF PARTICLES CONSIDERED 1146

MUON DISTRIBUTION  
 400 GEV INCIDENT  
 FIGURE 12

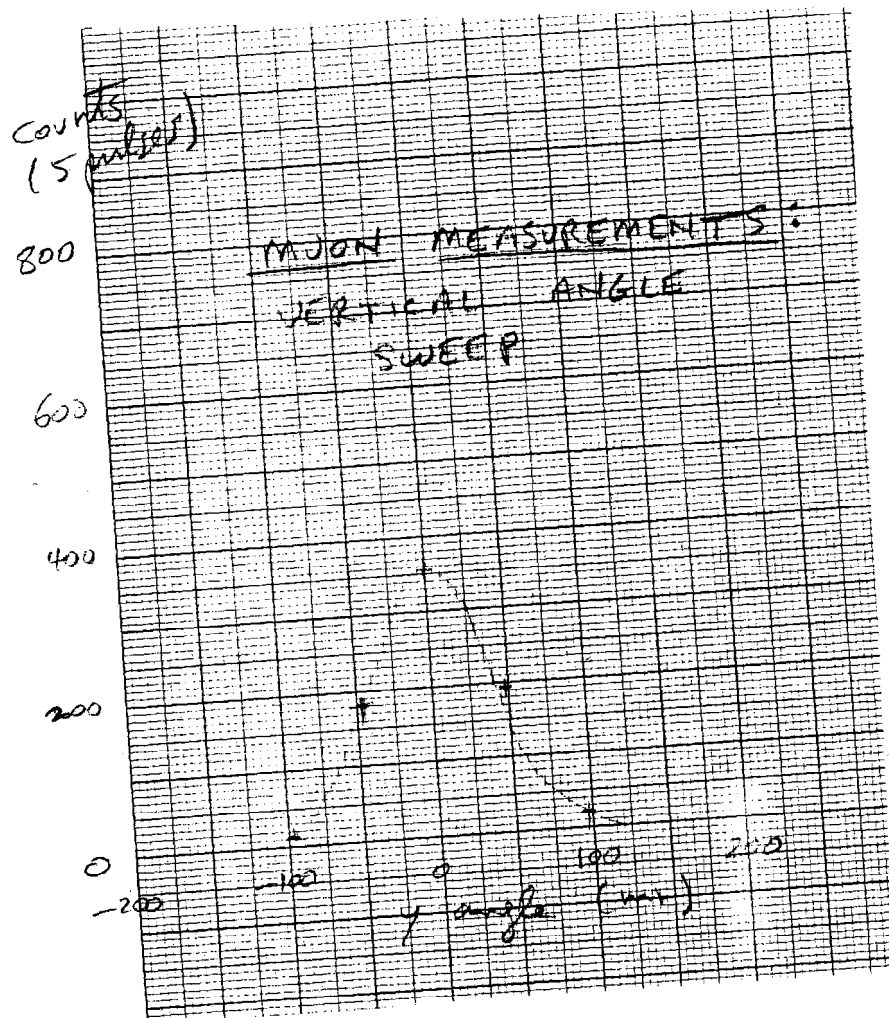
+ SUMS

1146

FIG. 13



ANGULAR WIDTH  
MUON MEASUREMENT  
FIG. 14

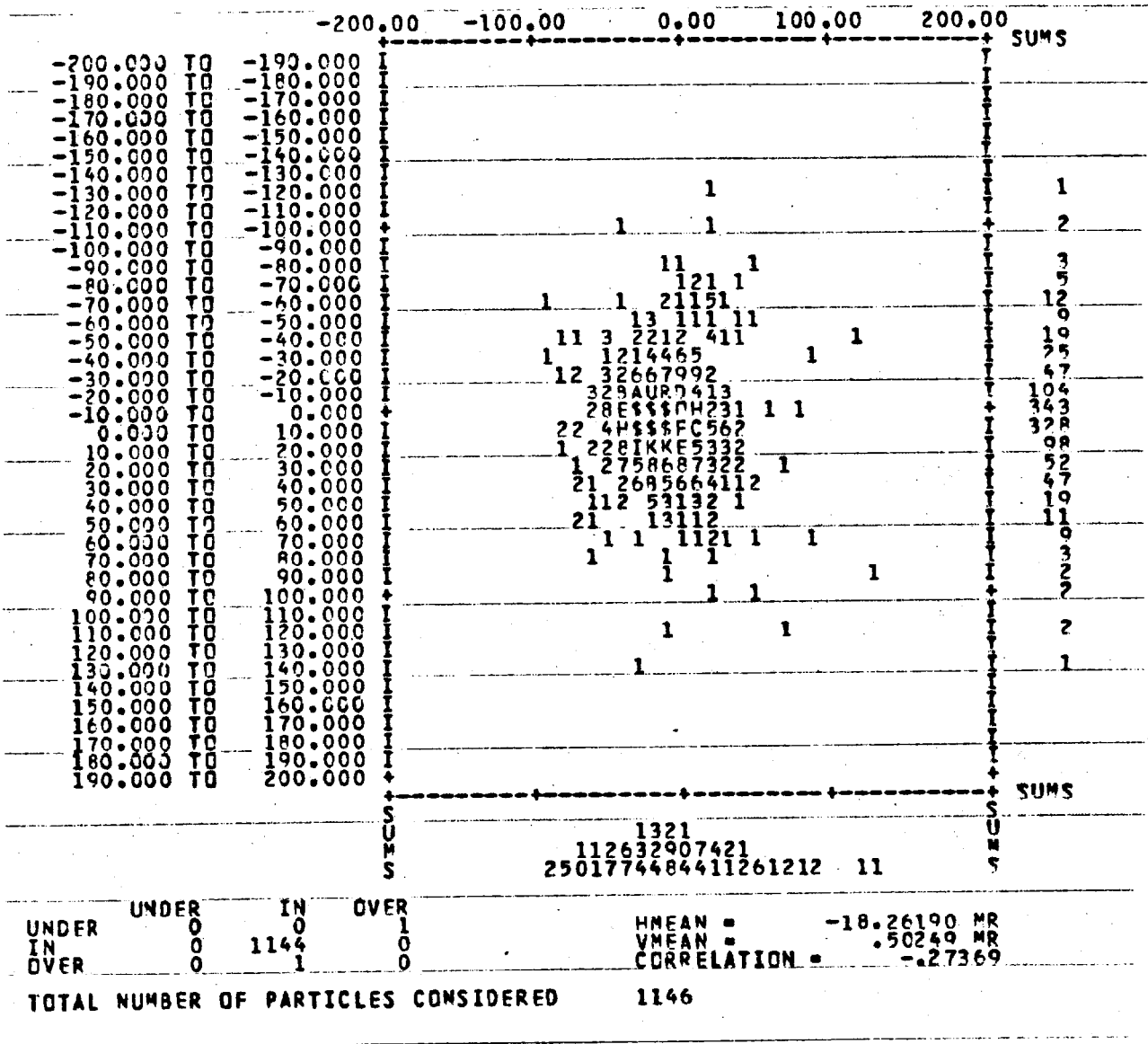


ANGULAR WIDTH  
MOON MEASUREMENTS

FIG. 15



HISTOGRAM NO. 2  
 HORIZONTAL AXIS... X' IN MR FOR HALO AT 1405.000 FT (POSITION 1)  
 VERTICAL AXIS... Y' IN MR FOR HALO AT 1405.000 FT (POSITION 1)



X', y' SCATTER PLOT  
 MUON CALCULATION  
 400 GEV INCIDENT

FIGURE 16